

Design and fabrication of an surface acoustic wave resonator based on AlN/4H-SiC material for harsh environments*

Wei-zhong WANG¹, Ji LIANG², Yong RUAN¹, Wei PANG², Zheng YOU^{1†‡}

⁽¹⁾Collaborative Innovation Center for Micro/Nano Fabrication, Device and System, State Key Laboratory of Precision Measurement Technology and Instruments, Department of Precision Instrument, Tsinghua University, Beijing 100084, China)

⁽²⁾State Key Laboratory of Precision Measurement Technology and Instruments, Tianjin University, Tianjin 300072, China)

[†]E-mail: yz-dpi@mail.tsinghua.edu.cn

Received Jan. 21, 2016; Revision accepted May 13, 2016; Crosschecked Dec. 12, 2016

Abstract: Surface acoustic wave (SAW) sensors and micro-electromechanical system (MEMS) technology provide a promising solution for measurement in harsh environments such as gas turbines. In this paper, a SAW resonator (size: 1107 $\mu\text{m} \times 721 \mu\text{m}$) based on the AlN/4H-SiC multilayer structure is designed and simulated. A MEMS-compatible fabrication process is employed to fabricate the resonator. The results show that highly c-axis-oriented AlN thin films deposited on the 4H-SiC substrate are obtained, with that the diffraction peak of AlN is 36.10° and the lowest full width at half maximum (FWHM) value is only 1.19° . The test results of the network analyzer are consistent with the simulation curve, which is very encouraging and indicates that our work is a significant attempt to solve the measurement problems mainly including high temperature stability of sensitive structures and the heat transmission of leads in harsh environments. It is essential to get the best performance of SAW resonator, optimize and characterize the behaviors in high temperatures in future research.

Key words: Surface acoustic wave (SAW) resonator; AlN/4H-SiC; Harsh environment; Micro-electromechanical system (MEMS) technology; Gas turbine

<http://dx.doi.org/10.1631/jzus.A1600028>

CLC number: TH703.2

1 Introduction

In core equipment such as gas turbines, high temperature measurements are urgently required to improve efficiency and to reduce emissions and maintenance costs (Pisano, 2009). But the harsh environment makes the sensors be made with costly wire harnesses, or even unrealizable (Thompson, 2004; You *et al.*, 2014). Recently, a new kind of sensing systems based on micro-electromechanical

system (MEMS) technology and surface acoustic wave (SAW) sensors classified as delay-line and resonator scores achieved high marks in harsh environments due to their desirable characteristics of no power, no wires, small size, low fabrication cost, ease of integration, and high sensitivity (Senesky *et al.*, 2009; Greve *et al.*, 2013). To summarize, MEMS SAW sensors, based on piezoelectric materials, are promising solutions for applications in harsh environments (Jiang *et al.*, 2013).

However, there are very few piezoelectric materials capable of withstanding high temperatures except Languisite (LGS, 1470°C), Gallium orthophosphate (GaPO_4 , 930°C), and Aluminium nitride (AlN, 1040°C), and only the layered structure AlN/substrate can be used for high frequencies ($>1 \text{ GHz}$)

[‡] Corresponding author

* Project supported by the Tsinghua University Initiative Scientific Research Program (No. 20131089351), China

 ORCID: Wei-zhong WANG, <http://orcid.org/0000-0001-6909-0110>

© Zhejiang University and Springer-Verlag Berlin Heidelberg 2017

(Elmazria and Aubert, 2011). Actually, there are many researchers studying SAW devices based on AlN/sapphire structures for high temperature applications (Aubert *et al.*, 2010; 2013). However, the sapphire substrate is difficult to process further, and it is incompatible with MEMS fabrication processes, which tremendously limits its use. Fortunately, the layered structure AlN/SiC could be an alternative solution.

SiC is a mechanically robust, chemically inert, and electrically stable wide-band gap semiconductor material. It does not have a melting point, and there is only a sublimation point of 2830 °C in harsh environments, mainly including the cubic 3C-SiC and hexagonal (4H-SiC and 6H-SiC) polytypes (Senesky, 2013; Fraga *et al.*, 2014). Recently, AlN thin films grown on 3C-SiC substrate have been characterized in high temperature environments (540 °C), and AlN shows good potential for long-term high-temperature stability (Lin *et al.*, 2013). But 3C-SiC and AlN (002) film have a lattice mismatch of 28.6% that needs to be addressed by a complicated two-step deposition process (Lin *et al.*, 2010a). In contrast, 6H-SiC and 4H-SiC are the most suitable substrates for AlN film due to their low lattice mismatch (0.96% and 1.2%, respectively) and their close thermal expansion coefficients (Liu and Edgar, 2002). Moreover, 4H-SiC is cheaper and easier for commercialization. Recently, although several research groups have focused on the deposition of AlN thin films onto 4H-SiC (Takagaki *et al.*, 2002) and 6H-SiC (Iriarte *et al.*, 2011) substrates, there is still no complete design and fabrication of SAW resonators based on AlN/4H-SiC material by radio frequency (RF) reactive magnetron sputtering for harsh environments.

Here, for the first time, we have designed and simulated a SAW resonator based on the AlN/4H-SiC multilayer structure. In addition, a MEMS-compatible fabrication process has been employed to fabricate the SAW resonator. The results show that highly c-axis-oriented AlN thin films deposited on the 4H-SiC substrates are obtained, with that the diffraction peak of AlN is 36.10° and the lowest full width at half maximum (FWHM) value is only 1.19°. Moreover, the testing results of the network analyzer are consistent with the simulation curve.

2 Design and fabrication of the SAW resonator

2.1 Operating principle of the SAW resonator

The operating principle of the SAW resonator is illustrated in Fig. 1. The wireless interrogation device emits a radio wave to activate SAW with the help of the inverse piezoelectric effect through an interdigital transducer (IDT) which is connected to an antenna. The two reflecting gratings reflect the SAW propagating along the piezoelectric substrate to form a resonator. Then the IDT transforms the SAW into a modulated radio wave to the wireless interrogation devices by the piezoelectric effect. On the other hand, once the structural parameters of the SAW resonator are determined, it has a unique resonance frequency at a definite temperature. In other words, the resonance frequency is a function of temperature (Liu *et al.*, 2014). As long as the frequency of the modulated radio wave is measured, the temperature value can be obtained, which makes the SAW resonator a potential temperature sensor.

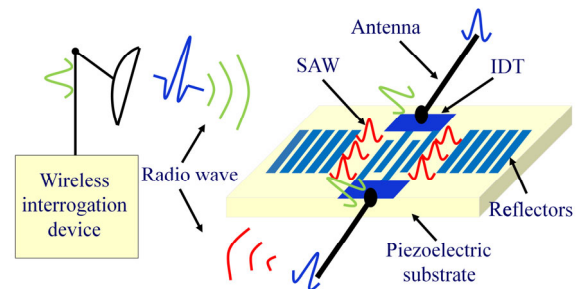


Fig. 1 Schematic diagram of the SAW resonator

2.2 Parameter design

The structural parameters of the SAW resonator are shown in Fig. 2. The resonant frequency of the SAW resonator can be calculated as

$$f = \frac{V_s}{\lambda_0}, \quad (1)$$

where V_s is the velocity of SAW in piezoelectric material, and λ_0 is the wavelength of SAW.

According to the principle of wave interference, only if the IDT pitch ($a+b$) is equal to the integer times (N) of half a SAW wavelength ($\lambda_0/2$), the

phase superposition and the strongest IDT excitation of SAW can be acquired, i.e.,

$$a + b = N \frac{\lambda_0}{2}. \quad (2)$$

In order to ensure that the IDT is on the peak of the standing wave, the distance of IDT and reflecting grating L_r must satisfy

$$L_r = \left(N - \frac{1}{2} \right) \frac{\lambda_0}{2}. \quad (3)$$

Besides, the transducer aperture also has an effect on the performance of the SAW resonator, and it is usually 50–100 times the wavelength (Ye *et al.*, 2011). In order to simplify and minimize the resonator, we make a equal b and set N to be 1. All the design parameters of the SAW resonator are summarized in Table 1.

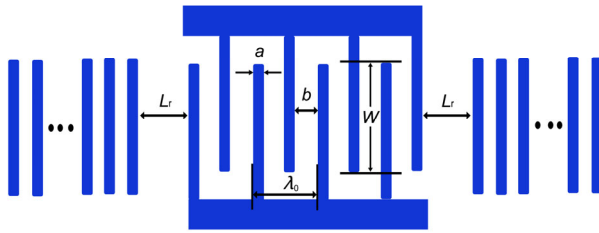


Fig. 2 Structural parameters of the SAW resonator

Table 1 Design parameters of the IDT and the reflecting grating of the SAW resonator

Parameter	Value
IDT electrode width, a (μm)	3
IDT electrode pitch, b (μm)	3
Transducer aperture, W (μm)	600
Number of IDT pairs, N_0	30
Number of reflecting grating pairs, N_1	62
Distance of IDT and reflecting grating, L_r (μm)	3
IDT electrode (Mo) thickness, t (nm)	100

2.3 Finite element simulation

The finite element simulation software COMSOL Multiphysics is used to simulate the device performance. Piezoelectric devices and eigenfrequency

are used to determine the resonance frequency of the SAW resonator and to calculate the velocity of the SAW in the AlN/4H-SiC structure.

The following constants of AlN are used in this study (Du, 2012). The elasticity matrix is

$$\mathbf{G}_E = \begin{bmatrix} 410 & 140 & 100 & 0 & 0 & 0 \\ 0 & 410 & 100 & 0 & 0 & 0 \\ 0 & 0 & 380 & 0 & 0 & 0 \\ 0 & 0 & 0 & 125 & 0 & 0 \\ 0 & 0 & 0 & 0 & 125 & 0 \\ 0 & 0 & 0 & 0 & 0 & 135 \end{bmatrix} \times 10^9 \text{ Pa}.$$

The coupling matrix is

$$\mathbf{e} = \begin{bmatrix} 0 & 0 & 0 & 0 & -0.48 & 0 \\ 0 & 0 & 0 & -0.48 & 0 & 0 \\ -0.58 & -0.58 & 1.55 & 0 & 0 & 0 \end{bmatrix} \text{ C/m}^2.$$

The relativity permittivity matrix is

$$\boldsymbol{\varepsilon} = \begin{bmatrix} 9 & 0 & 0 \\ 0 & 9 & 0 \\ 0 & 0 & 11 \end{bmatrix},$$

and the density is 3260 kg/m^3 .

In addition, elastic properties of 4H-SiC are defined as isotropic material properties with Young's modulus of 748 GPa and Poisson's ratio of 0.45, and density is 3216 kg/m^3 .

Periodic boundary conditions are used to dictate that the electric potential and displacements be the same along both vertical boundaries of the geometry. The simulated results show that the resonant and anti-resonant frequencies of the SAW resonator evaluate to approximately 647.13 and 651.68 MHz, respectively. Figs. 3a and 3b show the corresponding SAW modes, respectively. Thus, the corresponding velocity of SAW is 7765 m/s according to Eqs. (1) and (2).

2.4 MEMS fabrication

The fabrication techniques of AlN film on SiC substrate mainly include metal organic chemical vapor deposition (MOCVD) (Chen *et al.*, 2008),

plasma-assisted molecular beam epitaxy (MBE) (Ferro *et al.*, 2000), pulsed laser deposition (PLD) (Kim *et al.*, 2008), low-pressure hydride vapor phase epitaxy (LP-HVPE) (Kitagawa *et al.*, 2014), direct current (DC) reactive sputtering (Tungasmita *et al.*, 2000), and RF reactive sputtering (Kuang *et al.*, 2012). Because of low deposition temperature (about 400 °C), RF reactive magnetron sputtering is compatible with the MEMS process. Besides, a 99.999% pure aluminum target and a 99.999% pure nitrogen and argon gas mixture can be used to deposit AlN films of higher purity within shorter deposition time with a RF magnetron sputtering method. It also has the advantages of an easy process with a significant degree of freedom to adjust the process parameters, the ability for large-scale production with relatively low cost, etc. (Liu *et al.*, 2013), and it is regarded as one of the most promising methods. For the RF reactive magnetron sputtering coating process, process parameters, such as sputtering power, substrate temperature, sputtering pressure, target distance, the nitrogen concentration, and the substrate, have great influence on the preferred orientation of thin film and grain size and defects. After considering various influencing factors comprehensively and a sea of early experiments, we optimized the process parameters and completed the AlN film sputtering.

In addition, a MEMS-compatible resonator fabrication process has been employed, as illustrated in Fig. 4. It starts by depositing 2 μm AlN on the commercially available 4H-SiC wafer by RF sputtering deposition (Fig. 4a), and then 100 nm molybdenum is deposited by RF sputtering (Fig. 4b). After that, we patterned the IDT and the reflecting grating electrodes through photo lithography (Fig. 4c), and the SAW resonator was fabricated by wet etching at last (Fig. 4d).

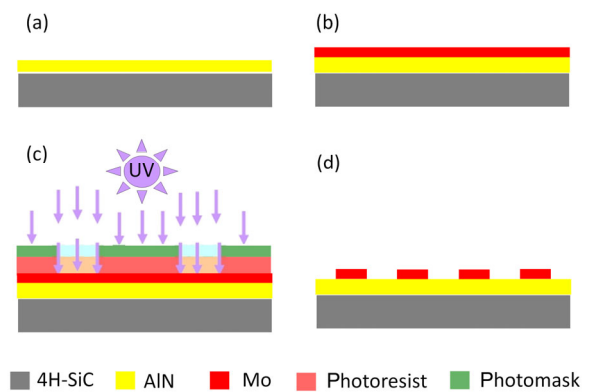


Fig. 4 Illustration of fabrication process

(a) AlN is deposited as piezoelectric layer on 4H-SiC; (b) Mo is deposited on AlN; (c) Mo is patterned through photo lithography; (d) IDT and reflecting grating electrode are fabricated by wet etching. UV: ultraviolet

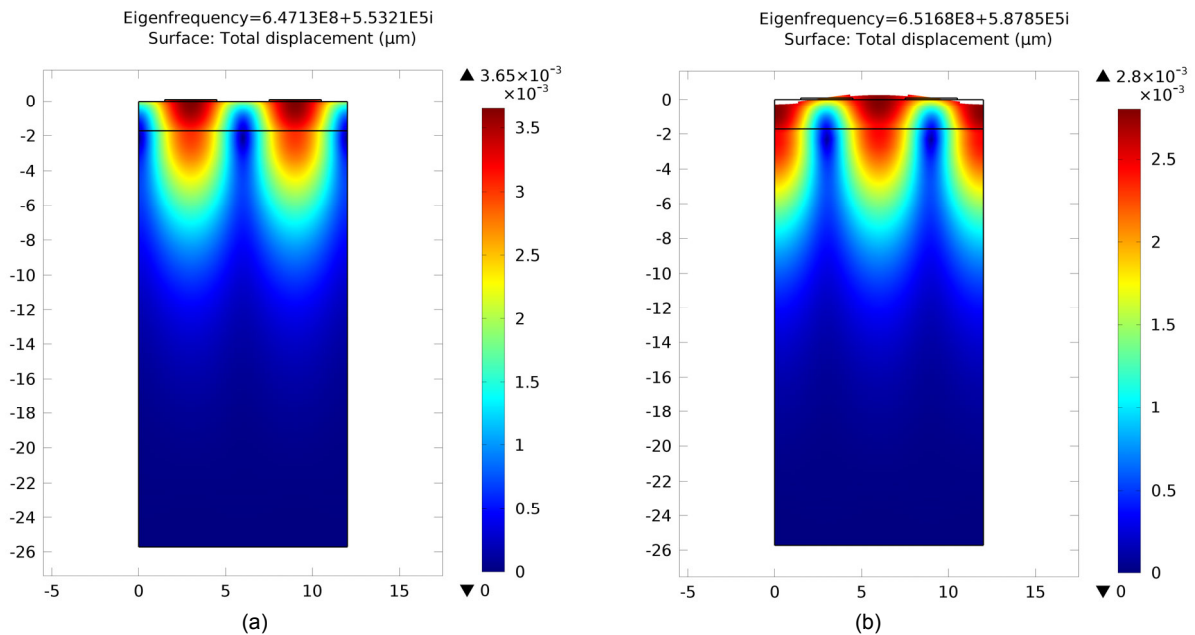


Fig. 3 Deformed shape plot of the resonant (a) and the anti-resonant (b) SAW modes on the AlN films and 4H-SiC (unit: μm)

3 Results and discussion

Fig. 5 shows the scanning electron microscopy (SEM) image of the AlN/4H-SiC multilayer structure where the AlN and 4H-SiC film thicknesses are 1.724 and 344 μm , respectively. Noting that there are errors between the actual thickness of the AlN and the design value of 2 μm , we altered the simulation parameters and did the simulation again to get the simulation results (Figs. 3 and 8). As shown in Fig. 5, the AlN thin film exhibits columnar grains perpendicular to the surface of the 4H-SiC layer, presenting high quality c-axis-oriented AlN thin film grown on the 4H-SiC layer. Furthermore, the crystalline structure was determined by the X-ray diffraction (XRD) as shown in Fig. 6 where the diffraction peak of AlN is 36.10° , and the X-ray diffraction rocking curve of the AlN film shows a FWHM value of 1.19° . The diffraction peak located at $2\theta=36.04^\circ$ is corresponding to (002) of ideal hexagonal AlN crystals, and for the FWHM value, the smaller the better (Wang *et al.*, 2011). Comparing the performance of the AlN developed with those reported in

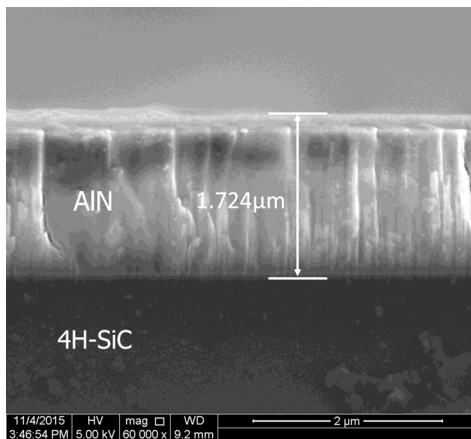


Fig. 5 Cross-sectional SEM micrographs of the 4H-SiC and AlN thin film

the literature shown in Table 2, the high crystalline quality AlN thin film was deposited on the 4H-SiC substrates.

Fig. 7 shows the fabricated resonator, where Fig. 7a is an optical image of the whole resonator (size: $1107 \mu\text{m} \times 721 \mu\text{m}$) and Fig. 7b is the optical image of the local details, indicating that as the etching in this method is a time-fixed etching, there is a little over etching of the Mo metal layer. But the final test results of the resonator in the next section prove that the processing error is within tolerance, or the resonator cannot be excited.

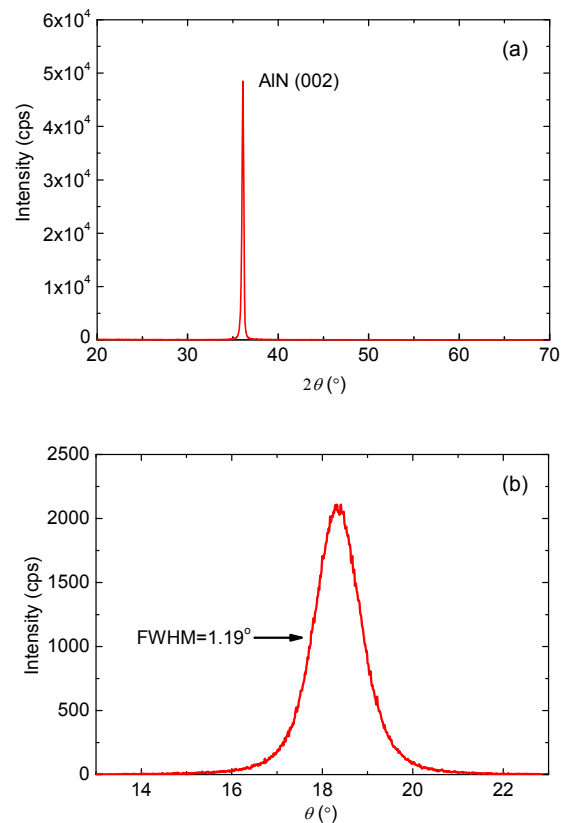


Fig. 6 XRD spectrum (a) and rocking curve (b) of the AlN film deposited on the 4H-SiC

Table 2 Performance of AlN thin film in literature

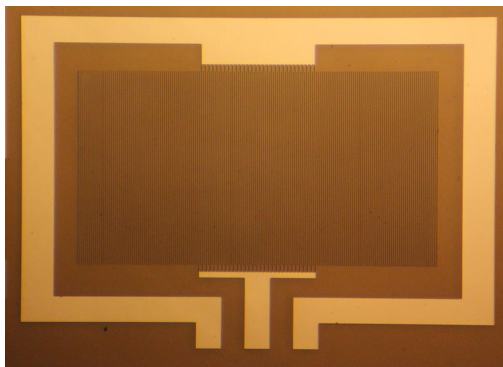
Substrate	Diffraction peak	FWHM	Processing method	Reference
4H-SiC	Around 36.04°	3.85°	Physical vapor deposition	Beshkova <i>et al.</i> , 2003
4H-SiC	Not given	2.47°	Metalorganic vapor phase epitaxy	Cho <i>et al.</i> , 2013
4H-SiC	Not given	0.64°	MOCVD	Al tahtamouni <i>et al.</i> , 2012
3C-SiC	Not given	1.73°	AC reactivemagnetron sputtering	Lin <i>et al.</i> , 2010b
SiC	Not given	1.37°	MOCVD	Chen <i>et al.</i> , 2008

The electrical performance of the SAW resonator is measured in a RF probe station at atmosphere pressure. Connected to an Agilent E5061B network analyzer, ground signal ground (GSG) probes are used to test the SAW resonator. After an open-short-load calibration, S11 parameters are extracted to get the frequency-impedance chart. S11 is measured directly by a network analyzer, which can be mutually transformed with the impedance Z_L by the following formulas:

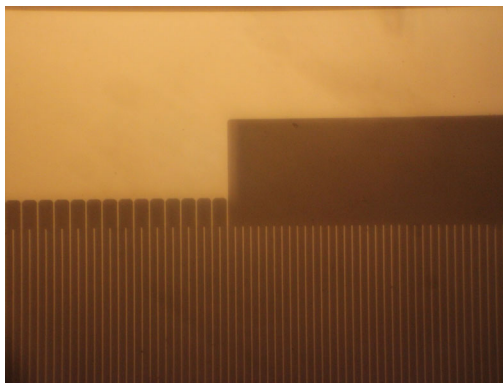
$$S11 = (1 + p) / (1 - p), \quad (4)$$

$$p = |Z_0 - Z_L| / (Z_0 + Z_L), \quad (5)$$

where p is the reflection coefficient, Z_0 is the characteristic impedance of 50Ω , and Z_L is the load impedance.



(a)



(b)

Fig. 7 Optical image of the fabricated resonator
(a) Whole structure; (b) Local details

Besides, the impedance is also simulated by Comsol. Fig. 8 shows the frequency-impedance chart of the finite element analysis (FEA) simulation and test results. In comparison with the simulation

curve, the test results of the network analyzer are consistent with it. There are many factors contributing to the margin of error between the simulation and test results. In the simulation, the material parameters are derived from the literature, not the actual resonator. In the resonator, not only the material parameters, but also the parasitic parameters, such as the parasitic capacitance, feed line inductance, and contact resistance, are key to verify the test results. Thus, it is very difficult to attribute to a particular factor. However, within the margin of error, it is clear enough to prove the correctness of the simulation and test results. In future research, it is essential to get the best performance of SAW resonator, and optimize and characterize the behaviors in high temperature.

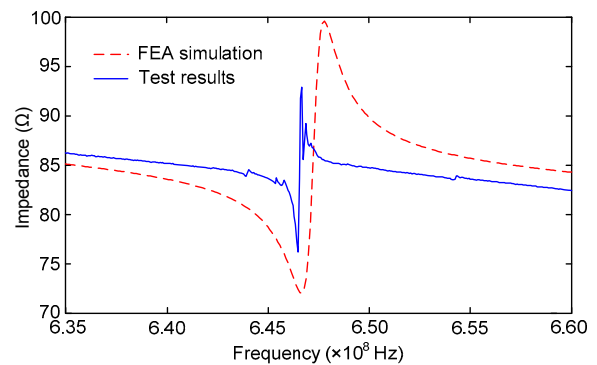


Fig. 8 Frequency-impedance chart of the FEA simulation and test results

4 Conclusions

For the first time, a SAW resonator (size: $1107 \mu\text{m} \times 721 \mu\text{m}$) based on the AlN/4H-SiC multi-layer structure is designed and fabricated in this study. Highly c-axis-oriented AlN thin films were successfully deposited on the 4H-SiC substrate by using RF reactive magnetron sputtering, and the lowest FWHM value is only 1.19° . All the structural parameters of the SAW resonator were determined, and the eigenfrequency and impedance were simulated by the finite element method. In addition, a MEMS-compatible fabrication process was employed to fabricate the SAW resonator. In comparison with the simulation curve, the test results of the network analyzer are consistent with it.

References

- Al tahtamouni, T.M., Lin, J.Y., Jiang, H.X., 2012. High quality AlN grown on double layer AlN buffers on SiC substrate for deep ultraviolet photodetectors. *Applied Physics Letters*, **101**(19):192106. <http://dx.doi.org/10.1063/1.4766732>
- Aubert, T., Elmazria, O., Assouar, B., et al., 2010. Surface acoustic wave devices based on AlN/sapphire structure for high temperature applications. *Applied Physics Letters*, **96**(20):203503. <http://dx.doi.org/10.1063/1.3430042>
- Aubert, T., Bardong, J., Legrani, O., et al., 2013. In situ high-temperature characterization of AlN-based surface acoustic wave devices. *Journal of Applied Physics*, **114**(1):014505. <http://dx.doi.org/10.1063/1.4812565>
- Beshkova, M., Zakhariev, Z., Birch, J., et al., 2003. Sublimation epitaxy of AlN layers on 4H-SiC depending on the type of crucible. *Journal of Materials Science: Materials in Electronics*, **14**(10):767-768. <http://dx.doi.org/10.1023/A:1026184600220>
- Chen, Z., Newman, S., Brown, D., et al., 2008. High quality AlN grown on SiC by metal organic chemical vapor deposition. *Applied Physics Letters*, **93**(19):191906. <http://dx.doi.org/10.1063/1.2988323>
- Cho, E., Mogilatenko, A., Brunner, F., et al., 2013. Impact of AlN nucleation layer on strain in GaN grown on 4H-SiC substrates. *Journal of Crystal Growth*, **371**:45-49. <http://dx.doi.org/10.1016/j.jcrysgro.2013.02.001>
- Du, X.Y., 2012. Design and Fabrication of a Prototype Aluminum Nitride-based Pressure Sensor with Finite Element Analysis and Validation. PhD Thesis, Wayne State University, Detroit, USA.
- Elmazria, O., Aubert, T., 2011. Wireless SAW sensor for high temperature applications: material point of view. SPIE Microtechnologies, International Society for Optics and Photonics, No.806602. <http://dx.doi.org/10.1117/12.889165>
- Ferro, G., Okumura, H., Yoshida, S., 2000. Growth mode of AlN epitaxial layers on 6H-SiC by plasma assisted molecular beam epitaxy. *Journal of Crystal Growth*, **209**(2-3):415-418. [http://dx.doi.org/10.1016/S0022-0248\(99\)00582-5](http://dx.doi.org/10.1016/S0022-0248(99)00582-5)
- Fraga, M.A., Furlan, H., Pessoa, R.S., et al., 2014. Wide band gap semiconductor thin films for piezoelectric and piezoresistive MEMS sensors applied at high temperatures: an overview. *Microsystem Technologies*, **20**(1):9-21. <http://dx.doi.org/10.1007/s00542-013-2029-z>
- Greve, D.W., Chin, T.L., Zheng, P., et al., 2013. Surface acoustic wave devices for harsh environment wireless sensing. *Sensors*, **13**(6):6910-6935. <http://dx.doi.org/10.3390/s130606910>
- Iriarte, G.F., Reyes, D.F., Gonzalez, D., et al., 2011. Influence of substrate crystallography on the room temperature synthesis of AlN thin films by reactive sputtering. *Applied Surface Science*, **257**(22):9306-9313. <http://dx.doi.org/10.1016/j.apsusc.2011.05.025>
- Jiang, X.N., Kim, K., Zhang, S.J., et al., 2013. High-temperature piezoelectric sensing. *Sensors*, **14**(1):144-169. <http://dx.doi.org/10.3390/s140100144>
- Kim, M., Ohta, J., Kobayashi, A., et al., 2008. Low-temperature growth of high quality AlN films on carbon face 6H-SiC. *physica status solidi (RRL)–Rapid Research Letters*, **2**(1):13-15. <http://dx.doi.org/10.1002/pssr.200701246>
- Kitagawa, S., Miyake, H., Hiramatsu, K., 2014. High-quality AlN growth on 6H-SiC substrate using three dimensional nucleation by low-pressure hydride vapor phase epitaxy. *Japanese Journal of Applied Physics*, **53**(5S1):05FL03. <http://dx.doi.org/10.7567/JJAP.53.05FL03>
- Kuang, X.P., Zhang, H.Y., Wang, G.G., et al., 2012. AlN films prepared on 6H-SiC substrates under various sputtering pressures by RF reactive magnetron sputtering. *Applied Surface Science*, **263**:62-68. <http://dx.doi.org/10.1016/j.apsusc.2012.08.121>
- Lin, C.M., Lien, W.C., Felmetsger, V.V., et al., 2010a. AlN thin films grown on epitaxial 3C-SiC (100) for piezoelectric resonant devices. *Applied Physics Letters*, **97**(14):141907. <http://dx.doi.org/10.1063/1.3495782>
- Lin, C.M., Lien, W.C., Yen, T.T., et al., 2010b. Growth of highly c-axis oriented AlN films on 3C-SiC/Si substrate. Solid-State Sensors, Actuators, and Microsystems Workshop, p.324-327.
- Lin, C.M., Chen, Y.Y., Felmetsger, V.V., et al., 2013. Surface acoustic wave devices on AlN/3C-SiC/Si multilayer structures. *Journal of Micromechanics and Microengineering*, **23**(2):025019. <http://dx.doi.org/10.1088/0960-1317/23/2/025019>
- Liu, B.Q., Zhang, C.R., Ji, X.J., et al., 2014. An improved performance frequency estimation algorithm for passive wireless SAW resonant sensors. *Sensors*, **14**(12):22261-22273. <http://dx.doi.org/10.3390/s14122261>
- Liu, H.Y., Tang, G.S., Zeng, F., et al., 2013. Influence of sputtering parameters on structures and residual stress of AlN films deposited by DC reactive magnetron sputtering at room temperature. *Journal of Crystal Growth*, **363**:80-85. <http://dx.doi.org/10.1016/j.jcrysgro.2012.10.008>
- Liu, L., Edgar, J.H., 2002. Substrates for gallium nitride epitaxy. *Materials Science and Engineering: R: Reports*, **37**(3):61-127. [http://dx.doi.org/10.1016/S0927-796X\(02\)00008-6](http://dx.doi.org/10.1016/S0927-796X(02)00008-6)

- Pisano, A.P., 2009. Harsh Environment Wireless MEMS Sensors for Energy & Power. Technical Report, Department of Electrical Engineering and Computer Science, University of California, Berkeley, USA.
- Senesky, D.G., 2013. Wide bandgap semiconductors for sensing within extreme harsh environments. *ECS Transactions*, **50(6)**:233-238.
<http://dx.doi.org/10.1149/05006.0233ecst>
- Senesky, D.G., Jamshidi, B., Cheng, K.B., et al., 2009. Harsh environment silicon carbide sensors for health and performance monitoring of aerospace systems: a review. *IEEE Sensors Journal*, **9(11)**:1472-1478.
<http://dx.doi.org/10.1109/JSEN.2009.2026996>
- Takagaki, Y., Santos, P.V., Wiebicke, E., et al., 2002. Superhigh-frequency surface-acoustic-wave transducers using AlN layers grown on SiC substrates. *Applied Physics Letters*, **81(14)**:2538-2540.
<http://dx.doi.org/10.1063/1.1509471>
- Thompson, H.A., 2004. Wireless and internet communications technologies for monitoring and control. *Control Engineering Practice*, **12(6)**:781-791.
<http://dx.doi.org/10.1016/j.conengprac.2003.09.002>
- Tungasmita, S., Birch, J., Persson, P.O.A., et al., 2000. Enhanced quality of epitaxial AlN thin films on 6H-SiC by ultra-high-vacuum ion-assisted reactive DC magnetron sputter deposition. *Applied Physics Letters*, **76(2)**:170-172.
<http://dx.doi.org/10.1063/1.125692>
- Wang, Z.P., Morimoto, A., Kawae, T., et al., 2011. Growth of preferentially-oriented AlN films on amorphous substrate by pulsed laser deposition. *Physics Letters A*, **375(33)**:3007-3011.
<http://dx.doi.org/10.1016/j.physleta.2011.06.043>
- Ye, X.S., Fang, L., Liang, B., et al., 2011. Studies of a high-sensitive surface acoustic wave sensor for passive wireless blood pressure measurement. *Sensors and Actuators A: Physical*, **169(1)**:74-82.
<http://dx.doi.org/10.1016/j.sna.2011.05.022>
- You, Z., Wang, W.Z., Chen, S., et al., 2014. Applications of wireless MEMS sensing system in gas turbine and harsh environment. *Acta Aeronautica et Astronautica Sinica*, **35(8)**:2081-2090 (in Chinese).
<http://dx.doi.org/10.7527/S1000-6893.2014.0084>

中文概要

题目: 面向恶劣环境的基于 AlN/4H-SiC 材料的声表面波谐振器设计与制作

目的: 在高温等恶劣工作环境下, 燃气轮机有着迫切的温度等工况参数的实时监测需求。声表面波 (SAW) 技术与微机电系统 (MEMS) 技术的结合可提供一种很有发展前景的解决方案。本文旨在探讨 SAW 谐振器的设计与仿真方法, 研究高质量 c 轴择优取向的 AlN 压电薄膜制备工艺及与 MEMS 工艺兼容的 SAW 谐振器制作工艺, 并测试其电学性能以验证 SAW 谐振器设计与制作的正确性与可行性。

创新点: 1. 首次在耐高温材料 AlN/4H-SiC 上设计、仿真及制作 SAW 谐振器并测试电学性能; 2. 在 4H-SiC 上得到了高质量 c 轴择优取向的 AlN 压电薄膜并开发了一套与 MEMS 工艺兼容的 SAW 谐振器制作工艺。

方法: 1. 通过对 SAW 谐振器所有结构参数的设计与仿真, 得到谐振器的谐振频率与反谐振频率等 (图 2 和 3); 2. 利用磁控溅射方法在 4H-SiC 衬底上溅射高质量 c 轴择优取向的 AlN 压电薄膜, 再利用光刻、湿法腐蚀等 MEMS 工艺制作 SAW 谐振器 (图 4); 3. 通过扫描电镜和 X 射线衍射等手段, 检测 AlN 压电薄膜质量 (图 5 和 6) 及器件制作结果 (图 7); 4. 利用网络分析仪测试 SAW 谐振器电学性能并与仿真结果相比较, 验证 SAW 谐振器设计仿真方法和 MEMS 制作工艺的可行性和有效性 (图 8)。

结论: 1. 基于耐高温材料 AlN/4H-SiC, 成功设计并制作出 SAW 谐振器 (尺寸: $1107 \mu\text{m} \times 721 \mu\text{m}$); 2. 在 4H-SiC 上得到了高质量 c 轴择优取向的 AlN 压电薄膜, 衍射峰为 36.10° , 摇摆曲线半高宽仅 1.19° ; 3. SAW 谐振器电学性能测试结果与仿真结果一致, 证明其设计仿真方法正确有效、MEMS 制作工艺可行。

关键词: SAW 谐振器; AlN/4H-SiC; 恶劣环境; MEMS 技术; 燃气轮机